

# Experimental determination of a time–temperature–transformation diagram of the undercooled $\text{Zr}_{41.2}\text{Ti}_{13.8}\text{Cu}_{12.5}\text{Ni}_{10.0}\text{Be}_{22.5}$ alloy using the containerless electrostatic levitation processing technique

Y. J. Kim,<sup>a)</sup> R. Busch, and W. L. Johnson

W. M. Keck Laboratory of Engineering Materials, California Institute of Technology,  
Pasadena, California 91125

A. J. Rulison<sup>b)</sup> and W. K. Rhim

Jet Propulsion Laboratory, California Institute of Technology, Pasadena, California 91109

(Received 8 September 1995; accepted for publication 13 December 1995)

High temperature high vacuum electrostatic levitation was used to determine the complete time–temperature–transformation (TTT) diagram of the  $\text{Zr}_{41.2}\text{Ti}_{13.8}\text{Cu}_{12.5}\text{Ni}_{10.0}\text{Be}_{22.5}$  bulk metallic glass forming alloy in the undercooled liquid state. This is the first report of experimental data on the crystallization kinetics of a metallic system covering the entire temperature range of the undercooled melt down to the glass transition temperature. The measured TTT diagram exhibits the expected “C” shape. Existing models that assume polymorphic crystallization cannot satisfactorily explain the experimentally obtained TTT diagram. This originates from the complex crystallization mechanisms that occur in this bulk glass-forming system, involving large composition fluctuations prior to crystallization as well as phase separation in the undercooled liquid state below 800 K.

© 1996 American Institute of Physics. [S0003-6951(96)03308-8]

The synthesis of bulk metallic glasses using low cooling rates was first achieved in the Ni–Pd–P alloy system.<sup>1,2</sup> Recently, after the discovery of several families of multicomponent alloys such as La–Al–Ni,<sup>3</sup> Zr–Al–Cu–Ni,<sup>4</sup> and Zr–Ti–Cu–Ni–Be,<sup>5</sup> bulk glass formation became a common phenomena. The undercooled liquid state of the latter alloy possesses an extremely high thermal stability with respect to crystallization. This lends the material to experimental study of its undercooling and solidification behavior. The containerless high-temperature high-vacuum electrostatic levitation (HTHVESL) processing technique<sup>6</sup> permits comprehensive studies of thermophysical properties in deeply undercooled liquid metals. By applying the HVHTESL technique to the  $\text{Zr}_{41.2}\text{Ti}_{13.8}\text{Cu}_{12.5}\text{Ni}_{10.0}\text{Be}_{22.5}$  alloy, for example, the authors found that proper thermal treatment during solidification results in the “self-fluxing” of the melt, allowing it to successfully undercool down to the glass transition with cooling rates of about 1 K/s.<sup>7</sup> Detailed thermodynamic studies were made to explain the stability of the undercooled liquid.<sup>8</sup> Thermophysical properties, such as specific heat capacity and total hemispherical emissivity, over the whole range of the undercooled liquid have been determined.<sup>9</sup>

Due to the limited glass-forming ability of earlier alloys, the acquisition of basic data on crystallization kinetics in the deeply undercooled melts has not been previously possible. However, the application of the HVHTESL technique to the  $\text{Zr}_{41.2}\text{Ti}_{13.8}\text{Cu}_{12.5}\text{Ni}_{10.0}\text{Be}_{22.5}$  alloy offers a new opportunity to study the crystallization kinetics in the entire undercooled melt down to the glass transition. In this letter, we report the experimental of the TTT diagram, which describes the occur-

rence of the crystallization events as a function of isothermal annealing time and temperature in the undercooled liquid. For the first time, we experimentally define the complete TTT diagram for the crystallization of an alloy for the whole range of the undercooled liquid, i.e., from the melting point down to the glass transition temperature.

The details of the alloy preparation steps and the experimental apparatus of the electrostatic levitator are described elsewhere.<sup>6,7</sup> The sample temperature was measured using an  $E^2T$  pyrometer (model 7000ET-1HR). Prior to the temperature measurements, the pyrometer was calibrated using the known eutectic temperature of 937 K. Initially, the molten sample was cooled radiatively to a predetermined temperature by blocking the heating source of a xenon arc lamp. Then, the iris of the xenon arc lamp was opened to maintain that temperature. Since the pyrometer measures the radiance of the sample at 4  $\mu\text{m}$  (nominally), the temperature measurements are accurate even in the presence of the UV-rich heating source for the entire isothermal treatment. The temperature fluctuations during isothermal treatments were within about  $\pm 5$  K, before recalescence due to crystallization occurred. The time required to initiate crystallization during the isothermal treatments was measured as the onset of recalescence.

Figure 1 shows a cooling curve obtained by purely radiative cooling.<sup>7</sup> The alloy did not crystallize during solidification as x-ray diffraction and differential scanning calorimetry (DSC) investigations revealed.<sup>7,9</sup> A small recalescence effect occurs below 800 K, which we attribute to a phase separation in the undercooled liquid state resulting in a small heat release.<sup>9</sup> This phase separation was confirmed by atom probe field ion microscopy (AP/FIM) measurements on samples cooled with a rate of approximately 10 K/s.<sup>10</sup> The schedule of the construction of the TTT diagram is added in Fig. 1, indicating the isothermal experiments to determine the time required to reach the onset of crystallization at dif-

<sup>a)</sup>Present address: Pohang University of Science and Technology, Department of Materials Science and Engineering, San 31, Hyozu-Dong, Pohang 790-784, Korea. Electronic mail: yjkim@vision.postech.ac.kr

<sup>b)</sup>Present address: Microgravity Programs, Space System/Loral, MS G38, Palo Alto, CA 94303-4604.

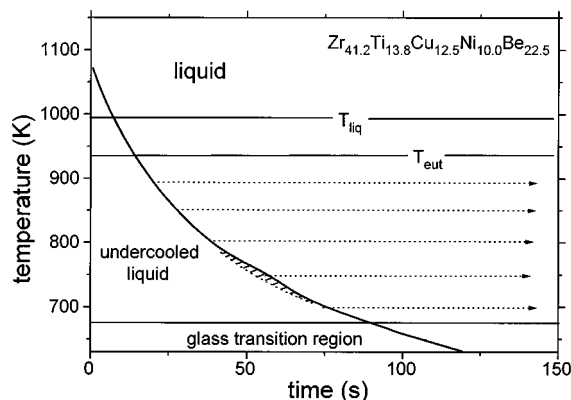


FIG. 1. Radiative cooling curve of a  $\text{Zr}_{41.2}\text{Ti}_{13.8}\text{Cu}_{12.5}\text{Ni}_{10.0}\text{Be}_{22.5}$  alloy that is undercooled below the liquidus temperature,  $T_{\text{liq}}$ , and the eutectic temperature,  $T_{\text{eut}}$ . Below 800 K, a small recalescence event is observed (hatched line) that we attribute to the decomposition of the undercooled liquid with respect to Zr and Be. The schedules for the isothermal measurements to determine the TTT diagram (dotted) are added in the plot.

ferent isothermal temperatures. Prior to each isothermal measurement, the sample alloy was subjected to melting and radiative cooling cycles shown in Fig. 1 to ensure a clean sample (i.e., “self-fluxing”), so that heterogeneous nucleation could be avoided.<sup>7</sup> The time origin (i.e.,  $t=0$ ) was defined to be the time at which the sample temperature reaches the melting point of 993 K during radiative cooling. The time required for crystallization of the undercooled liquid during isothermal treatments is much longer than the total time for vitrification shown in Fig. 1, as will be demonstrated.

A temperature–time profile for moderate undercooling below the melting point is shown in Fig. 2(a), indicating the isothermal treatment and the recalescence due to the crystallization, which heated the sample up to the eutectic temperature of 937 K. At this degree of undercooling, only a single crystallization event is observed. Figure 2(b), in contrast, shows a temperature–time profile in which the sample was cooled about 200 K deeper until phase separation took place (area I). The subsequent annealing at 730 K led to a primary crystallization with an onset time of 360 s (area II) and a secondary crystallization at an onset time of 800 s (area III). The primary crystallization peak from the metastable undercooled liquid is rather broad and around 400 s long, suggesting a copious nucleation event but sluggish growth kinetics. After the completion of primary crystallization, the remaining undercooled liquid crystallized, as indicated by a sharper second heat release event which is about 200 s long.

Based on DSC experiments, AP/FIM results,<sup>10</sup> and transmission electron microscopy and small angle neutron scattering studies,<sup>11</sup> we believe that for these undercoolings a phase separation (event I) into Be-poor and Be-rich regions precedes the nucleation of crystals. According to Schneider *et al.*,<sup>11</sup> the primary crystallization (event II) can be attributed to the formation of a nanocrystalline Be-poor and Ti-rich f.c.c. phase, which is embedded in a noncrystalline Be-rich matrix. This implies that during the time period of 360 s between event I and II an additional decomposition involving Ti has to occur [Fig. 2(b)]. During the secondary crystallization (event III) the remaining Be-rich supercooled liquid

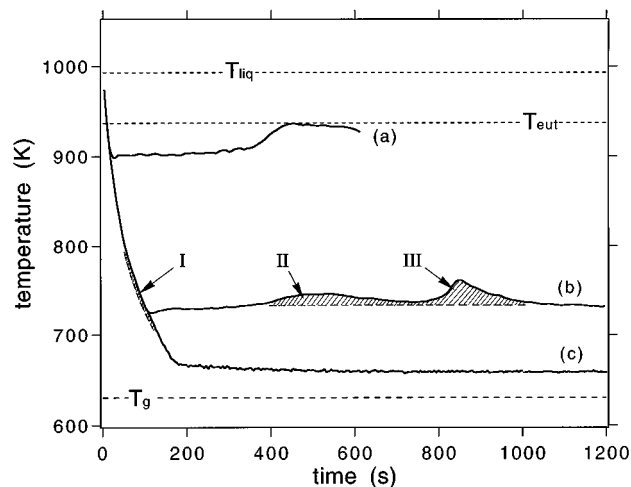


FIG. 2. Temperature–time profiles for different undercoolings below the melting point. Curve (a) shows the isothermal treatment at 900 K and the recalescence that leads to a temperature increase up to 937 K. In curve (b), a sample is undercooled down to 730 K, where phase separation (area I) occurs. Subsequently, the sample crystallizes in two events (areas II+III). Curve (c) shows a time–temperature profile of a sample that is undercooled down to 670 K where no recalescence is observed. The onset of the glass transition for a heating rate of 1.667 K/s is added ( $T_g$ ).

crystallizes as well. It should be noted that the total heat release for the observed decomposition (100–200 J/g atom) with respect to Be and Zr is much smaller than the overall heat release for the crystallization events (approximately 5.5 kJ/g atom).<sup>8</sup> The ultimate crystallization, however, also involves an additional phase separation with respect to Ti.<sup>11</sup> At an annealing temperature of 660 K, shown in Fig. 2(c), no crystallization event was observed. Implying that the kinetics in the metastable undercooled liquid is too sluggish to develop crystallization within the time scale of the experiment.

Figure 3 summarizes all the measured times for the onset of crystallization at various isothermal temperatures as a TTT diagram. It shows the typical “C” shape, as expected, with a “nose” of the TTT curve at 51 s and 850 K. This temperature of the nose, however, is relatively high in comparison with the predictions of conventional models for the TTT curves, as will be discussed below. The critical cooling rate to bypass the “nose” (i.e., crystallization) is 1.8 K/s, which is consistent with previous experimental results.<sup>7</sup> Figure 3 also indicates that crystallization of the metastable undercooled liquid is dominated by one crystallization event above 800 K, whereas below 800 K primary (⊗) and secondary crystallization (●) is observed as the result of the preceding phase separation in the undercooled liquid state.

It is of interest to compare the conventional models with the measured TTT diagram to evaluate the kinetics analyses (i.e., TTT diagram) combined with the classical nucleation and growth theory of crystalline phases in an undercooled liquid. We have made several attempts to fit the measured TTT curves using, for example, the Uhlmann<sup>12</sup> and Davis<sup>13</sup> kinetic formulations. Even with the use of recent specific heat capacity<sup>8</sup> and viscosity data,<sup>14</sup> we were not successful in fitting the high lying “nose” feature with conventional kinetic models. These deviations are very likely due to the unreasonable estimates of the homogeneous nucleation

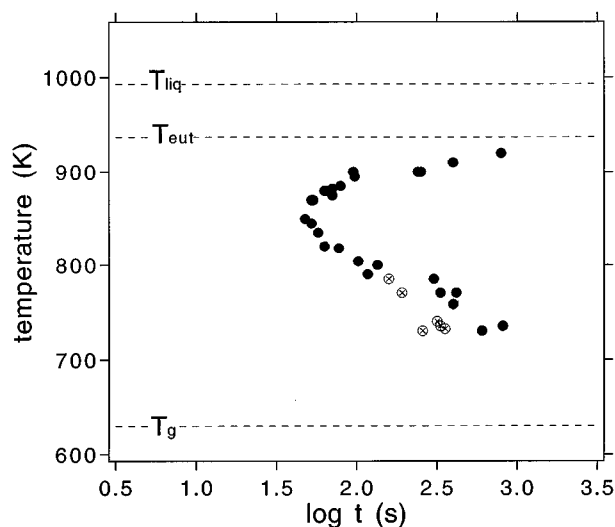


FIG. 3. Time-temperature-transformation diagram reflecting the onset of crystallization as a function of undercooling (●). Below 800 K two crystallization events are observed. The primary crystallization (⊗) is followed by secondary crystallization (●).

rate. In fact, the above models for the kinetics and others<sup>15</sup> are based on the assumption of a polymorphic transformation. However, multicomponent alloys such as the  $\text{Zr}_{41.2}\text{Ti}_{13.8}\text{Cu}_{12.5}\text{Ni}_{10.0}\text{Be}_{22.5}$  alloy used in this investigation, in general, do not follow a simple polymorphic transformation to the crystalline state. If the composition of the initial homogeneous melt is substantially different from the composition of the crystals formed upon primary crystallization, long range diffusion of one or more components must occur to produce the necessary concentration fluctuation. For the  $\text{Zr}_{41.2}\text{Ti}_{13.8}\text{Cu}_{12.5}\text{Ni}_{10.0}\text{Be}_{22.5}$  alloy, this is the case above about 800 K, where no tendency to phase separation is observed. In the presence of a miscibility gap (below 800 K) the additional decomposition process has to be taken into account. There are at least two factors to be considered to account for the high “nose” observed in the TTT diagram of the alloy. First, the time scale required to produce a concentration fluctuation will have a complex dependence on temperature. With increasing undercooling, the diffusion constant decreases and the viscosity increases, respectively, leading to an increasingly longer time scale for building up a composition fluctuation. Furthermore, the observed phase separation in the undercooled liquid below 800 K implies that the restoring force for concentration fluctuations depends on temperature and may change sign with undercooling. Desré has discussed the role of concentration fluctuations in multicomponent alloys on crystal nucleation.<sup>16</sup> These effects are not included in the assumption of polymorphic crystallization. Second, the kinetics formulas do not include the compositional-dependent activation energy barrier to initiate the nucleation. Barrier crossing in multicomponent alloys is in fact a complex problem involving correlated fluc-

tuations of composition and topological nucleus growth. Wu<sup>17</sup> and others<sup>18–21</sup> have discussed this problem. More detailed analyses combined with the experimental data are in progress to explain the disagreement between experimental results and the conventional models based on the classical theory on nucleation and growth of crystalline phases.

In this letter, we demonstrated an experimental technique to determine TTT diagram for crystallization of undercooled bulk glass forming  $\text{Zr}_{41.2}\text{Ti}_{13.8}\text{Cu}_{12.5}\text{Ni}_{10.0}\text{Be}_{22.5}$  liquids. To achieve these data, containerless electrostatic levitation was applied. For the first time, a TTT diagram for the transformation from the liquid state into the solid state was constructed experimentally in the whole undercooled liquid range for a metallic melt. The measured diagram exhibits a significantly higher “nose” temperature compared to the calculated diagram based on the classical theories that assume polymorphic solidification. This observation is not surprising, since this multicomponent alloy shows a very complex crystallization behavior involving large concentration fluctuations of several alloy components as well as phase separation at temperatures lower than 800 K.

The authors wish to thank S. K. Chung for his help and gratefully acknowledge the support of the National Aeronautics and Space Administration (Grant Nos. NAG8-954 and NAS49619201063550), the Department of Energy (Grant No. DEFG-03-86ER-45242), and the Alexander von Humboldt Foundation via the Foedor Lynen Program. Part of the work was carried out at the Jet Propulsion Laboratory, California Institute of Technology, under contract with the National Aeronautics and Space Administration.

- <sup>1</sup> H. W. Kui, A. L. Greer, and D. Turnbull, *Appl. Phys. Lett.* **45**, 615 (1984).
- <sup>2</sup> H. W. Kui and D. Turnbull, *Appl. Phys. Lett.* **47**, 796 (1985).
- <sup>3</sup> A. Inoue, T. Zhang, and T. Masumoto, *Mater. Trans. JIM* **31**, 425 (1991).
- <sup>4</sup> T. Zhang, A. Inoue, and T. Masumoto, *Mater. Trans. JIM* **32**, 1005 (1991).
- <sup>5</sup> A. Peker and W. L. Johnson, *Appl. Phys. Lett.* **63**, 2342 (1993).
- <sup>6</sup> W. K. Rhim, S. K. Chung, D. Barber, K. F. Man, G. Gutt, A. J. Rulison, and R. E. Spjut, *Rev. Sci. Instrum.* **64**, 2961 (1993).
- <sup>7</sup> Y. J. Kim, R. Busch, W. L. Johnson, A. J. Rulison, and W. K. Rhim, *Appl. Phys. Lett.* **65**, 2136 (1994).
- <sup>8</sup> R. Busch, Y. J. Kim, and W. L. Johnson, *J. Appl. Phys.* **77**, 4039 (1995).
- <sup>9</sup> R. Busch, Y. J. Kim, W. L. Johnson, A. J. Rulison, W. K. Rhim, and D. Isheim, *Appl. Phys. Lett.* **66**, 3111 (1995).
- <sup>10</sup> R. Busch, S. Schneider, A. Peker, and W. L. Johnson, *Appl. Phys. Lett.* **67**, 1544 (1995).
- <sup>11</sup> S. Schneider, P. Thiyagarajan, and W. L. Johnson, *Appl. Phys. Lett.* **68**, 493 (1996).
- <sup>12</sup> D. R. Uhlmann, *J. Non-Cryst. Solids* **25**, 43 (1977).
- <sup>13</sup> H. A. Davis, *Phys. Chem. Glasses* **17**, 159 (1976).
- <sup>14</sup> E. Bakke, R. Busch, and W. L. Johnson, *Appl. Phys. Lett.* **67**, 3260 (1995).
- <sup>15</sup> F. Spaepen and D. Turnbull, in *Rapidly Quenched Metals II*, edited by N. J. Grant and B. C. Giessen (MIT Press, Cambridge, MA, 1976), p. 205.
- <sup>16</sup> P. J. Desré, *Proceedings of the International Conference on Non-Crystalline Materials*, Grenoble, France (1994), to be published in *Mater. Sci. Forum*.
- <sup>17</sup> D. T. Wu, *J. Chem. Phys.* **99**, 1990 (1993).
- <sup>18</sup> H. Reiss, *J. Chem. Phys.* **18**, 840 (1950).
- <sup>19</sup> V. O. Hirschfelder, *J. Chem. Phys.* **35**, 2690 (1974).
- <sup>20</sup> D. Stauffer, *J. Aerosol Technol.* **7**, 319 (1976).
- <sup>21</sup> H. Trinkhaus, *Phys. Rev. B* **27**, 7372 (1983).